Monopoles, confinement, and deconfinement of (2+1)D compact lattice QED in external fields

M. N. Chernodub*

ITEP, B. Cheremushkinskaya 25, Moscow, 117259, Russia

E.-M. Ilgenfritz[†]

Institut für Theoretische Physik, Universität Tübingen, D-72076 Tübingen, Germany

A. Schiller[‡]

Institut für Theoretische Physik and NTZ, Universität Leipzig, D-04109 Leipzig, Germany

The compact Abelian model in three space-time dimensions is studied in the presence of external electromagnetic fields at finite temperatures. We show that the deconfinement phase transition is independent of the strength of the external fields. This result is in agreement with our observation that the external fields create small-size magnetic dipoles from the vacuum which do not influence the confining properties of the model. Contrary to the deconfinement phase, the internal field in the direction of the applied external field is attenuated in the confinement phase; this screening becomes stronger with decreasing temperature.

I. INTRODUCTION

Compact Abelian gauge theory in three Euclidean dimensions is proven to possess the property of permanent confinement [1,2] due to presence of Abelian monopoles: any pair of test electric charge and anticharge are confined by a linear potential. The monopoles are topological defects which appear due to the compactness of the gauge group. In three dimensions the monopoles are instantonlike.

The confining property of the model is lost at sufficiently high temperature. The confinement-deconfinement phase transition—which is expected [3–5] to be of the Kosterlitz-Thouless type [6]—was studied on the lattice both analytically [5] and numerically [4]. A thorough numerical analysis of the phase transition was done in Ref. [7] where it has been demonstrated that the monopoles are sensitive to the transition. In the confinement phase the monopoles are observed in the plasma state while in the deconfinement phase the monopoles appear in the form of a dilute gas of magnetic dipoles. Similarly to the monopole plasma the dipole vacuum, although not confining, still has a nonperturbative nature [8]. In the confinement phase both monopole density and string tension differ from semiclassical estimates [1] which neglect monopole binding. However, an analysis of monopole clusters shows that the relation between the string tension and the density of monopoles in *magnetically charged* clusters is in reasonable agreement with those predictions.

An alternative explanation of the deconfinement phase transition, based on Svetitsky-Yaffe universality arguments [3], was given in Refs. [4,5]. The phase transition was demonstrated to be accompanied by restructuring of the $U(1)$ vortex system in an effective two-dimensional (2D) Abelian spin model. In the confinement (low temperature) phase the

vortices exist in the plasma state while in the deconfinement (high temperature) phase the vortices and antivortices form bound states. Both monopole [9] and vortex [10] binding mechanisms have been studied in the context of the Georgi-Glashow model, too, a limiting case of which is the compact Abelian gauge model.

In this paper we continue to consider the deconfining mechanism by monopole pairing which seems to have interesting counterparts in realistic gauge theories. The formation of monopole pairs is qualitatively similar to the binding of instantons in instanton molecules with increasing temperature in QCD suggested to be responsible for chiral symmetry restoration [11]. An external magnetic field affects the phase diagram of the non-Abelian theory as was shown both analytically [12] and numerically [13]. In the electroweak theory, the formation of Nambu monopole-antimonopole pairs, a remnant from a dense medium of disordered Z vortices and Nambu monopoles which characterizes the high temperature phase, is accompanying the transition towards the low temperature phase [14]. The effects of the external fields on the phase transition temperature and the electroweak baryogenesis in the electroweak theory were discussed in Ref. [15].

In three-dimensional gauge theories the inclusion of external fields allows to study the vacuum energy density in the $SU(2)$ gauge theory [16], vortex dynamics in the Abelian Higgs model [17], and dynamically generated fermion mass in the Abelian gauge theory with fermionic [18] fields. Here we study the influence of the external electromagnetic field on the confining and monopole properties of the compact Abelian gauge model in three dimensions.

The plan of the paper is as follows. In Sec. II we describe the basics of the lattice formulation of the compact $U(1)$ model in $2+1$ dimensions and how the external field is implemented. The screening of the external electric and magnetic fields and the properties of the Polyakov loop correlators in the presence of those fields are studied in Sec. III. Differences and similarities between magnetic and electric

————————

*Email address: maxim@heron.itep.ru

[†]Email address: ilgenfri@alpha1.tphys.physik.uni-tuebingen.de

[‡]Email address: Arwed.Schiller@itp.uni-leipzig.de

fields are stressed. The string tension in the presence of the external fields with a flux n_{ext} is investigated in Sec. IV and the phase diagrams in the n_{ext}-β plane are presented in Sec. V, separately for magnetic and electric fields. In the case of an applied electric field we see that the so-called "bulk Polyakov loop" can no longer play the usual role in localizing the deconfining transition. Results for various monopole properties are collected in Sec. VI. Our conclusions are summarized in the last section.

II. THE COMPACT LATTICE MODEL IN EXTERNAL FIELDS

We study $(2+1)$-dimensional compact lattice electrodynamics in constant external electromagnetic fields. Following Ref. [19] we use the action

$$S[\theta, \theta^{ext}] = -\beta \sum_p \cos(\theta_p - \theta_p^{ext}), \qquad (2.1)$$

where θ_p is the $U(1)$ field strength tensor represented by the curl of the compact link field θ_l, and θ_p^{ext} is the field strength corresponding to the external field. β is the lattice coupling constant related to the lattice spacing a and the continuum coupling constant g_3 of the 3D theory as follows:

$$\beta = \frac{1}{a\, g_3^2}. \qquad (2.2)$$

At finite temperature the lattice is asymmetric, $L_s^2 \times L_t$, $L_t < L_s$; $L_1 = L_2 = L_s$ and $L_3 = L_t$ are the spatial and temporal extensions of the lattice, respectively. In the limit $L_s \rightarrow \infty$ the temporal extension of the lattice L_t is related to the physical temperature, $L_t = 1/(Ta)$. Using Eq. (2.2) the temperature is given via the lattice parameters as follows:

$$\frac{T}{g_3^2} = \frac{\beta}{L_t}. \qquad (2.3)$$

Note that in $2+1$ dimensions there is no symmetry anymore between the three components of the field strength tensor. The closest relative of the true magnetic field is F_{12} distinct from the others, while there is still a symmetry between F_{13} and F_{23}. With this distinction in mind one can conditionally call them the "magnetic" and "electric" components of the field strength tensor, respectively. As long as one does not introduce external fields, even at finite temperature there was no need to distinguish between them.

Without loss of generality we represent an external electric field E as a field directly coupled via Eq. (2.1) to plaquettes lying in the 31 plane. The value of the field is quantized [19]:

$$E = \theta_{31}^{ext} = \frac{2\pi n_E}{L_1 L_3}, \quad n_E \in \mathbb{Z}, \quad \theta_{12}^{ext} = \theta_{23}^{ext} = 0. \qquad (2.4)$$

To study the influence of a magnetic field (and to draw parallels to analogous studies in four dimensions [20]) we

implement a magnetic field B as a field directly coupled via Eq. (2.1) to plaquettes lying in the 12 plane,

$$B = \theta_{12}^{ext} = \frac{2\pi n_M}{L_1 L_2}, \quad n_M \in \mathbb{Z}, \quad \theta_{31}^{ext} = \theta_{23}^{ext} = 0. \qquad (2.5)$$

The quantization of the external fields (2.4) and (2.5) is necessary to match with the periodic boundary conditions imposed on the lattice [19]. Indeed, these conditions imply that the rectangular Wilson loop of the size $L_i \times L_j$ in the ij plane must be equal to unity. On the other hand the Wilson loop is equal to $\exp\{i\Phi\}$, where Φ is the flux going through the ij plane. Therefore, we get the quantization condition for the flux, $\Phi = 2\pi n_{ext}$, $n_{ext} \in \mathbb{Z}$, which implies in turn the relations (2.4) and (2.5) for the constant electric or magnetic field, respectively. We use the notation $n_{E/M}$ instead of n_{ext} where we want to emphasize the electric/magnetic nature of the external field.

Naturally, from the form of the action (2.1) the number of external fluxes is restricted, $0 < n_{ext} < L_i L_j / 2$. In our analysis we restrict that number to $0 < n_{ext} < L_i L_j / 4$. One should note, however, that the largest considered fluxes correspond to lattice artifacts. Indeed, the physical electromagnetic field must have a strength smaller than the scale corresponding to the lattice ultraviolet cutoff, a^{-2}. This leads to the restriction of the lattice field strength: $\theta_{ext} \ll 1$, or $n_{ext} \ll n_{max} = [L_i L_j/(2\pi)]$, to avoid too large external fields.

As in the case of zero field [7] we restrict ourselves to a finite temperature lattice $32^2 \times 8$ varying the strength of the constant external electric or magnetic field and considering the lattice gauge coupling range $0.1 \leq \beta \leq 3$. For this particular lattice size we get the upper bounds for the electric and magnetic fields: $n_E^{max} = 40$ and $n_M^{max} = 163$, respectively. From our studies at zero external fields we [7] found the deconfinement phase transition at $\beta_c = 2.346(2)$ using the Polyakov loop susceptibility in satisfactory agreement with Ref. [4].

We briefly recall the Monte Carlo algorithm used and described already in Ref. [7]. The algorithm combines a local Monte Carlo step with a global refreshment step to improve ergodicity. The local Monte Carlo algorithm is based on a five-hit Metropolis update sweep followed by a microcanonical sweep. Following Ref. [19], the global refreshment step consists of an attempt to add an additional unit of flux of randomly chosen direction and sign (i.e., adding a gauge field $\tilde{\theta}_i$ constructed over the whole lattice to the previous one $\theta_i \rightarrow [\theta_i + \tilde{\theta}_i]_{mod 2\pi}$), subject to a global Metropolis acceptance check. The acceptance rate for a global update does not depend on the external flux n_{ext} and it is roughly equal for global shifts of the electric or magnetic flux. However, it changes with β, reducing from $0.58 \cdots 0.6$ at $\beta = 1.0$ to $0.18 \ldots 0.20$ at $\beta = 2.9$.

III. POLYAKOV LOOP CORRELATORS AND SCREENING

Usually, the Polyakov loop

$$L(\mathbf{x}) = \exp\left\{ i \int_0^{L_t} dt\, A_0(\mathbf{x}, t) \right\} \qquad (3.1)$$

is used as the basic quantity to probe the confining properties. The integration runs along a loop $l_{\mathbf{x}}$ parallel to the time axis and located at the spatial 2D coordinate $\mathbf{x}$. The Polyakov loop operator inserts an infinitely heavy test particle with unit electric charge into the vacuum of the theory. The vacuum expectation value (VEV) of this operator expresses the free energy F of the inserted particle, $\langle L(\mathbf{R}) \rangle = \exp(-F/T)$ and is an order parameter to signal deconfinement.

In the absence of an external field the correlation function between two Polyakov loops can be expressed via the interaction potential $V(R)$ between infinitely heavy electric charge and anticharge,

$$\langle L(\mathbf{0}) L^*(\mathbf{R}) \rangle \propto \exp\{-L_t V(\mathbf{R})\}. \tag{3.2}$$

The leading behavior of the potential $V(\mathbf{R})$ in the low temperature phase corresponds to a linearly rising potential, $V(R) = \sigma R$, where σ is the tension of the string between the test electric charges separated by the distance $R = |\mathbf{R}|$. In the high temperature phase the potential is of Coulomb type (it rises logarithmically with increasing distance between test particles).

Now we discuss the Polyakov loop correlations in both electric and magnetic external fields. We introduce a 3D vector combining electric and magnetic components by

$$\vec{F} = (F_{23}, F_{31}, F_{12}) = (E_x, E_y, B_z). \tag{3.3}$$

As we will immediately see, an external (constant) electric field substantially modifies the behavior of the Polyakov loop correlator (3.2) already *on the tree level*.

Indeed, the electromagnetic field inside the medium can be decomposed into two parts, $\vec{F}^{\text{int}} + \vec{F}^q$. Here $\vec{F}^{\text{int}}$ is the mean field inside the medium, which is nonzero due to the presence of the external electromagnetic field. The field $\vec{F}^q$ corresponds to the quantum fluctuations around the mean value $\vec{F}^{\text{int}}$. Because of the Abelian nature of the Polyakov loop the correlation function (3.2) can be written as the product of two contributions,

$$\langle L(\mathbf{0}) L^*(\mathbf{R}) \rangle_{\vec{F}^{\text{ext}}} = \left\langle \exp\left\{ i \oint_{\mathcal{C}} dx_\mu A_\mu(x) \right\} \right\rangle_{\vec{F}^{\text{ext}}}$$

$$= e^{i\Phi_{\mathcal{C}}(\vec{F}^{\text{int}})} \cdot G(\mathbf{R}, \vec{F}^{\text{ext}}), \tag{3.4}$$

$$G(\mathbf{R}, \vec{F}^{\text{ext}}) = \langle L(\mathbf{0}) L^*(\mathbf{R}) \rangle_{\vec{F}^{\text{ext}}}^q = \langle e^{i\Phi_{\mathcal{C}}(\vec{F}^q)} \rangle_{\vec{F}^{\text{ext}}}^q, \tag{3.5}$$

where $\mathcal{C} = l_{\mathbf{0}} - l_{\mathbf{R}}$ is the contour corresponding to the test particle trajectories, and

$$\Phi_{\mathcal{C}}(\vec{F}) = \oint_{\mathcal{C}} dx_\mu A_\mu(x) = \int_{\Sigma_{\mathcal{C}}} d\sigma_\mu F_\mu(x) \tag{3.6}$$

is the flux of the electromagnetic field F which goes through the surface $\Sigma_{\mathcal{C}}$ spanned on the contour $\mathcal{C}$. The subscript $\vec{F}^{\text{ext}}$ in Eq. (3.5) indicates that the vacuum expectation value of the quantum part of the Polyakov loop has been taken with the action Eq. (2.1) corresponding to nonzero external flux.

The correlator (3.5) is taken over quantum fluctuations only, as indicated by the superscript q. Note that by definition the field A^q fluctuates near the minimum of the action. Thus negative modes are absent and the potential $V(\mathbf{R}; \vec{F}^{\text{ext}}) \propto -\ln G(\mathbf{R}, \vec{F}^{\text{ext}})/L_t$ must be real. The dynamics of the monopoles affects the quantum fluctuations and consequently the potential V. The external fields disturb the monopole medium and therefore we may expect that in general the interparticle potential V may get influenced by the external fluxes.

Summarizing, the quantum average of the Polyakov loop in the presence of the external constant electromagnetic field is given by the following formula:

$$\langle L(\mathbf{0}) L^*(\mathbf{R}) \rangle_{\vec{F}^{\text{ext}}} \propto \exp\{i\Phi_{\mathcal{C}}(\vec{F}^{\text{int}}) - L_t V(\mathbf{R}; \vec{F}^{\text{ext}})\}, \tag{3.7}$$

where a *nonvanishing* flux $\Phi_{\mathcal{C}}(\vec{F}^{\text{int}})$ pierces the surface $\Sigma_{\mathcal{C}}$ spanned by the contour $\mathcal{C}$ and the trajectories of the test particles are placed along the (temporal) z direction.

The properties of the internal fields inside the system are important to understand the behavior of the Polyakov loop correlators. For external fields given by Eqs. (2.4) and (2.5) the total external fluxes through the corresponding planes are quantized. Analogously, the internal electric or magnetic fluxes through any plane in any gauge field configuration are quantized as well (the considerations similar to those in Sec. II are applicable in this case as well). Note that the global update step is consistent with the internal flux quantization since the update allows to change the total flux of the system by just one unit.

From now on we study only two possibilities for the external field, an electric field in the y direction and a magnetic field in the z direction,

$$\vec{F}^{\text{ext}} = (0, E, 0), \quad \text{or} \quad \vec{F}^{\text{ext}} = (0, 0, B). \tag{3.8}$$

It is clear that only the electric component contributes to the flux $\Phi_{\mathcal{C}}(\vec{F}^{\text{int}})$ in Eq. (3.7). In our case the mean internal electric and magnetic fields which are the actual average fields present in the medium are given by $\langle \theta_{31} \rangle$ and $\langle \theta_{12} \rangle$, respectively, where

$$\langle \theta_{ik} \rangle = \left\langle \frac{1}{L_s^2 L_t} \sum_x [\theta_{x,ik}]_{\text{mod}2\pi} \right\rangle. \tag{3.9}$$

Following Ref. [21] we show in Fig. 1 the normalized average internal electromagnetic fields $\langle \theta_{31} \rangle / E = F_2^{\text{int}}/E$ and $\langle \theta_{12} \rangle / B = F_3^{\text{int}}/B$ along the directions of the applied fields as a function of the gauge coupling β for various external field fluxes n_{ext}. One can see that in the confinement phase the internal fields are much weaker than the external fields while in the deconfinement phase the internal and external fields almost coincide with each other. The measured average internal fields in the directions transverse to the applied external field remain zero.

The attenuation of the external fields in the confinement phase resulting in weaker average fields in the medium happens due to the monopole plasma [1] and can be called
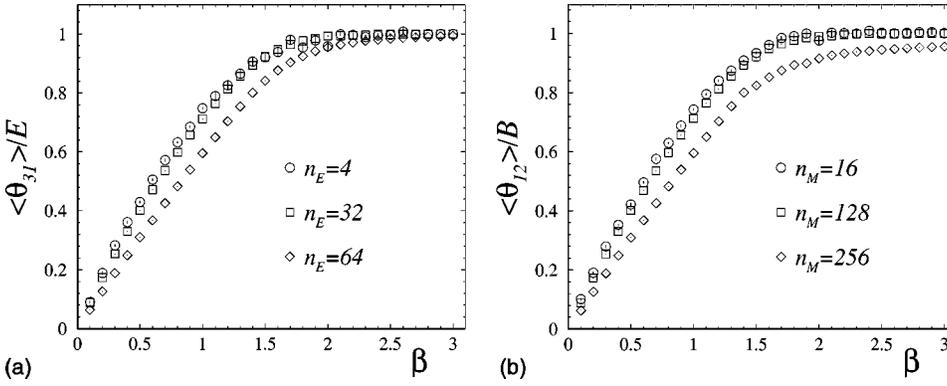
FIG. 1. The normalized internal (a) electric and (b) magnetic fields vs β at fixed n_{ext}.

screening: the monopoles produce a finite correlation length ξ. If we would apply an external field to the box with the monopole plasma using frozen boundary conditions then the field would be greatly suppressed inside the media at distances (from the box boundaries) larger than ξ. Thus the averaged field inside the box with the plasma should be smaller than the external field. The smaller the correlation length the smaller should be the averaged field inside the media.

As the temperature increases, the monopoles form more and more magnetic dipole bound states. In the dipole plasma the screening is absent [22] and the correlation length is infinite. The internal field is expected to be equal to the external one, which is clearly seen in Fig. 1 for external fields of small strength. Moreover, the screening of the external magnetic and electric fields with the same strength (related to each other as $n_E = n_M/4$ due to a difference in the lattice extensions in spatial and temporal directions) is very similar for weak external fields. This happens because the nature of the monopoles is not purely "magnetic" at finite temperature. At large magnetic fields the response of the media is different in magnetic and electric cases. In Sec. VI we show that the observed features of the screening are qualitatively related to specific properties of the monopoles and their bound states.

Let us consider the properties of the correlator (3.7) on a lattice of finite size for a nonvanishing external electric field E using the lattice Polyakov loop at position $\mathbf{x} = (x, y)$,

$$L(\mathbf{x}) = \exp\left(i \sum_{z=1}^{L_t} \theta_3(\mathbf{x}, z) \right). \tag{3.10}$$

We put the test charge and anticharge at the points $(0,0)$ and (x,y), respectively. The fluxes $\Phi_{\mathcal{C}}(\theta_{31})$ going through the surface $\Sigma_{\mathcal{C}}$ spanned between the test particle trajectories depend on the internal electric field θ_{31}; they are quantized and peaked around an average value. Therefore, they can adequately be described by taking into account only the "most probable" flux state labeled by the integer $n_{\text{int}} = n_{\text{int}}(n_{\text{ext}}, \beta, L_i)$ which depends on the strength of the external field, temperature, and lattice geometry. In that case $\Phi_{\mathcal{C}} = 2\pi n_{\text{int}} x / L_s$ and $E_{\text{int}} = \langle \theta_{31} \rangle = 2\pi n_{\text{int}}/(L_s L_t)$. The Polyakov loop correlator reads as follows,

$$\langle L(0,0) L^*(x,y) \rangle_E \propto \exp\left\{ 2\pi i n_{\text{int}} \frac{x}{L_s} - L_t V(x,y;E) \right\}, \tag{3.11}$$

with the oscillating part of the correlator defined by the electric component of the internal field.

Equation (3.11) simultaneously characterizes both the screening of the external field (phase factor) and the potential of the test electric charges (modulus). We expect that in the deconfinement phase the external field is not screened and the correlator is dominated by $n_{\text{int}} \approx n_E$. In the confinement phase the field must be screened and n_{int} becomes smaller with decreasing β (temperature).

Thus the Polyakov correlator in the deconfinement phase is an oscillating sign–changing quantity at a fixed y coordinate as a function of the x coordinate. The maxima of the oscillations become damped with increasing x due to the Coulombic interaction between the test particles.

The correlations at fixed x and changing y should be of the same sign and decay with increasing y. This behavior is nicely illustrated by the (real part of) the Polyakov loop correlators (3.11) in the x-y plane shown in Fig. 2(a) for the deconfinement phase. The measurement was performed in an external electric field with flux $n_E = 4$.

In the confinement phase we expect that the sign fluctuations of the correlator should be strongly suppressed due to area-law decay. Thus the correlator must go to zero rapidly with increasing distance between charge and anticharge, $\sqrt{x^2 + y^2}$. The corresponding correlator, presented in Fig. 2(b) at $\beta = 2.0$, shows the expected suppression. In addition, we observe a small local maximum at $x \approx 8$ and $y = 0$ arising from a flux of value n_{int} close to 4 in agreement with the behavior of the internal fields in Fig. 1 for this relatively large β value.

Finally, let us comment here that an induced internal magnetic field (parallel to its parental external field) which is directed *along* the Polyakov loop cannot contribute to the "classical" phase $\Phi_{\mathcal{C}}$ and, therefore, oscillations cannot appear. Thus, in an external magnetic field, the correlator is rapidly approaching zero with increasing spatial distance.

IV. STRING TENSION IN THE PRESENCE OF FIELDS

According to Ref. [23] the point-point correlation of the two Polyakov loops in the absence of an external field can be
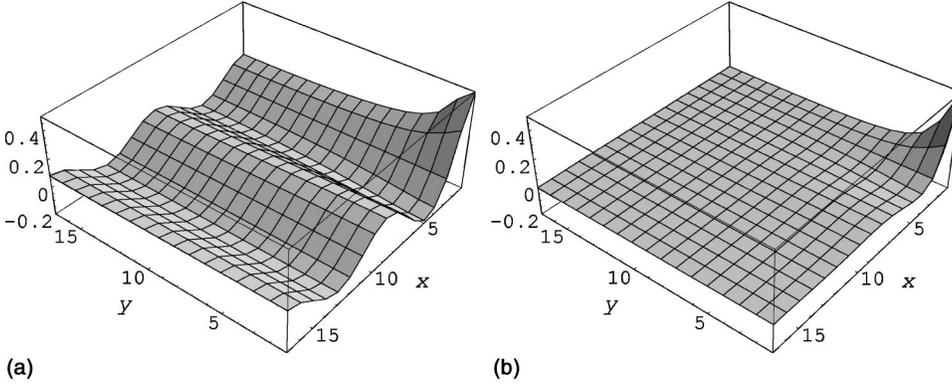
FIG. 2. Real part of the Polyakov loop correlator in the x-y plane (3.11) for an external electric flux $n_E=4$ in (a) deconfinement, $\beta=2.6$ and (b) confinement, $\beta=2.0$ phases. Half of the lattice $32^2\times 8$ is shown.

(a)   **(b)**

parametrized as follows:[1]

$$\langle L(x_1,y_1)L^*(x_2,y_2)\rangle$$

$$=\text{const}\sum_{p_{1,2}}\frac{e^{ip_1(x_1-x_2)+ip_2(y_1-y_2)}}{1-\cos p_1-\cos p_2+\cosh(\sigma L_t)}+\cdots,$$

(4.1)

where the sum runs over all possible momenta, $p_{1,2}=0,\ldots,2\pi(L_s-1)/L_s$ and σ denotes the "temporal" string tension.

To evaluate the string tension, we use two Polyakov "plane" operators which are defined as a sum over Polyakov loop positions along and perpendicular to the external field. As an example we take the electric field in the y direction. Then

$$L_{\parallel}(x)=\sum_{y=1}^{L_s}L(x,y),\quad L_{\perp}(y)=\sum_{x=1}^{L_s}L(x,y).$$

(4.2)

The correlator of the plane-plane correlators may be written as a sum over the corresponding positions of the point-point correlation functions,

$$\langle L_{\parallel}(0)L_{\parallel}^*(x)\rangle=\sum_{y_{1,2}=1}^{L_s}\langle L(0,y_1)L^*(x,y_2)\rangle,$$

(4.3)

$$\langle L_{\perp}(0)L_{\perp}^*(y)\rangle=\sum_{x_{1,2}=1}^{L_s}\langle L(x_1,0)L^*(x_2,y)\rangle.$$

(4.4)

In the presence of an electric field E along the y axis this correlator must be modified in accordance with our discussion in Sec. III,

———————

[1] Here and below we take into account only the lowest "mass state" corresponding to the actual string tension, unless specified otherwise.

$$\langle L(x_1,y_1)L^*(x_2,y_2)\rangle\to\langle L(x_1,y_1)L^*(x_2,y_2)\rangle_E$$

$$=\exp\left(-2\pi in_{\text{int}}\frac{x_1-x_2}{L_s}\right)\langle L(x_1,y_1)L^*(x_2,y_2)\rangle_{n_E}^q.$$

(4.5)

The subscript n_E indicates that the Polyakov loops are calculated in the state with an external electric flux n_E in the y direction. The internal electric flux n_{int} depends implicitly on that external flux. Combining Eqs. (4.1) and (4.5) with Eqs. (4.3) and (4.4) and taking the sums over the momenta $p_{1,2}$ explicitly, we get

$$\langle L_{\parallel}(0)L_{\parallel}^*(x)\rangle_{n_E}=\text{const}\times e^{2\pi in_{\text{int}}x/L_s}\cosh\left[\sigma L_t\left(x-\frac{L_s}{2}\right)\right],$$

(4.6)

$$\langle L_{\perp}(0)L_{\perp}^*(y)\rangle_{n_E}=\text{const}\times\cosh\left[\sigma_{\text{eff}}(\sigma,n_{\text{int}})L_t\left(y-\frac{L_s}{2}\right)\right],$$

(4.7)

where formally a string tension coefficient $\sigma_{\text{eff}}(\sigma,n_{\text{int}})$ for the plane-plane correlator perpendicular to the field has been defined:

$$\sigma_{\text{eff}}(\sigma,n_{\text{int}})=\frac{1}{L_t}\text{arccosh}[\cosh(\sigma L_t)-\cos(2\pi n_{\text{int}}/L_s)+1].$$

(4.8)

Thus in the presence of an external electric field the plane-plane Polyakov loop correlator parallel to the electric field oscillates with a decreasing amplitude.

The plane-plane correlator perpendicular to the field decreases exponentially (without oscillations) as a function of the distance between the planes. The decrease of this correlator is controlled by an *effective* string tension (4.8) which is a function of the external electric field (via n_{int}) and the actual string tension. The essential message here is that this effective string tension does not tell anything about confinement properties, since the confinement is described by the real string tension σ. Note that the effect of the external electric field is absent if the internal flux is equal to quantized values,
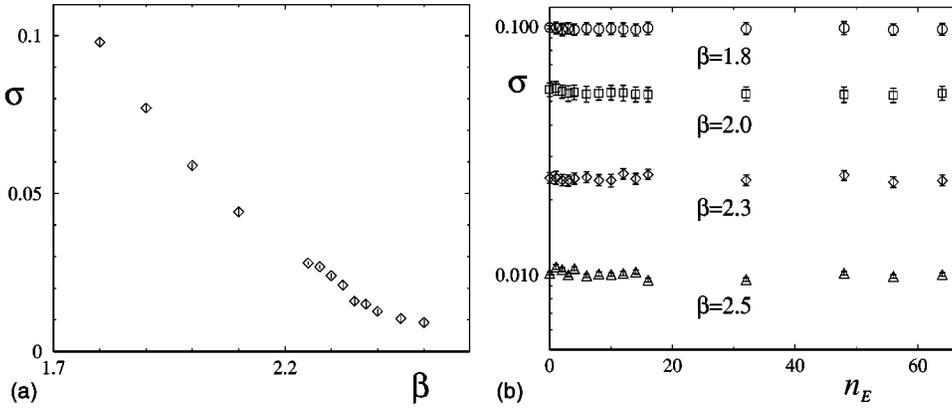
$$n_{\text{int}}=N\cdot L_s,\quad N\in\mathbb{Z}.$$

(4.9)

FIG. 3. (a) The string tension vs β without external field taken from Ref. [7]. (b) Fitted string tension for various β values as function of the external electric flux n_E.

The origin of the σ_{eff} dependence on the external electric field strength is related to the oscillatory behavior of the Polyakov loop correlator (3.11). Indeed, the bulk correlator $\langle |L|^2 \rangle_E$ [defined below in Eq. (5.1)] comprises all possible Polyakov loop correlators. At small and increasing n_{int} the sum of the oscillating quantities leads to a suppression of $\langle |L|^2 \rangle_E$ while at n_{int} satisfying the special condition (4.9) the oscillations disappear and as a result the effective string tension (4.8) coincides with the string tension in the absence of the external electric field.

To get rid of the direct influence of the electric field on the string tension (4.8) we use only the real part of the Polyakov plane-plane correlator which is parallel to the external field. We fit the numerical data by the real part of Eq. (4.6) using (besides trivial prefactors) σ and $n_{\text{int}} \in \mathbb{Z}$ as fitting parameters. At the considered values of $\beta \geqslant 1.6$ we find that the best fit is given by $n_{\text{int}} = n_{\text{ext}}$ in accordance with our discussion in Sec. III.

In the absence of external fields, the dependence of the string tension on β has been found in Ref. [7] and it is shown in Fig. 3(a). The string tension is a rapidly decreasing function: it is nonzero in the low temperature phase (low β) and becomes very small (due to finite size effects) in the high temperature phase. From Fig. 3(b) we conclude that within errors the string tension does not depend on the external flux n_E. This observation allows us to conclude that an external electric field in the compact $(2+1)$D Abelian gauge theory does not change the confinement behavior compared to the zero-field case.

For an external magnetic field (in the "temporal" z direction) the oscillating factor in the Polyakov loop correlator is absent. Therefore, we have used Eq. (4.6) with $n_{\text{int}} = 0$ to fit the plane-plane correlation functions of the Polyakov lines. The numerical results for the string tension σ are similar to those in the case of the electric field shown in Fig. 3(b): within errors of the fit values we do not observe a dependence of the string tension on the strength of the external field. Therefore we do not show the plot of the string tension vs the external magnetic flux.

Summarizing, both magnetic and electric fields do not influence the string tension. This fact is analyzed in terms of the monopole properties in Sec. VI. Before doing so we discuss the phase structure of the model using the Polyakov loop expectation value and the corresponding susceptibility.

V. PHASE STRUCTURE

The confinement-deconfinement phase transition is usually detected using the Polyakov loop vacuum expectation value. It is convenient to study VEV's of the powers of the "bulk Polyakov loop" defined as follows:

$$\langle |L| \rangle = \frac{1}{L_s^2} \left\langle \left| \sum_{\mathbf{x}} L(\mathbf{x}) \right| \right\rangle, \quad \langle |L|^2 \rangle = \frac{1}{L_s^2} \left\langle \left| \sum_{\mathbf{x}} L(\mathbf{x}) \right|^2 \right\rangle$$

$$= \frac{1}{L_s^2} \left\langle \sum_{\mathbf{x},\mathbf{y}} L(\mathbf{x}) L^+(\mathbf{y}) \right\rangle. \tag{5.1}$$

The Polyakov loop susceptibility is expressed via these quantities:

$$\chi_L = \langle |L| \rangle^2 - \langle |L|^2 \rangle. \tag{5.2}$$

According to the free energy arguments in the deconfinement phase the quantity $|L|$ should be nonvanishing while in the confinement phase this quantity becomes small (it approaches zero in the infinite volume limit).

In the following we show that the expectation value of the Polyakov loop, similar to the correlator discussed above, also gets a large classical contribution due to the external electric field. Therefore it should not be used in general as an order parameter to probe the restoration of confinement (except for some special values of the electric field).

A. Electric field

The behavior of the Polyakov loop vs β at various values of the external electric field is shown in Fig. 4(a). The plot of the Polyakov loop at zero field agrees with general expectations. However, as the electric field is turned on, the vacuum expectation value of the Polyakov loop is decreasing. One might conclude that the external electric field restores the confinement phase (while being in deconfinement at $n_E = 0$) which is in clear contradiction with the results for the string tension shown in the previous section. We remind the reader that the external electric field modifies the properties of the Polyakov loop correlator classically. In particular, for not too large n_E, it enhances what we called the *effective* string tension measured from the Polyakov plane-plane correlators perpendicular to the electric field [cf. Eq. (4.8)]. But,
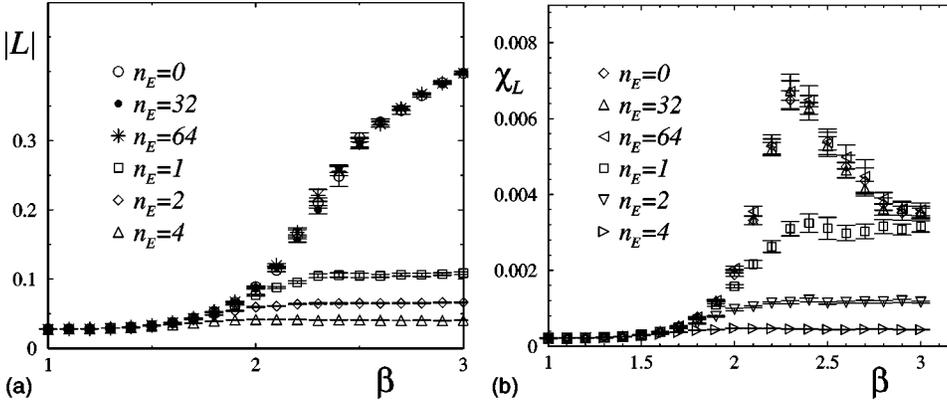
FIG. 4. (a) The absolute value of the bulk Polyakov loop (5.1) and (b) the Polyakov loop susceptibility (5.2) vs β for various values of the external electric field, n_E.

as we noted above, this effective string tension does not describe the confining properties of the system.

Thus we may conclude that the rapid decrease of the Polyakov loop as a function of n_E also does not mean that confinement is restored. Note that at large special values of the internal flux n_{int}, Eq. (4.9), the module of the Polyakov loop and the susceptibility [Fig. 4(b)] as a function of β do not differ from the zero-field case.

Let us estimate the classical correction to the Polyakov loop expectation value due to the external electric field E. For this purpose we consider the squared modulus of the Polyakov line, Eq. (5.1). In the presence of E it can be written as follows:

$$\langle |L|^2 \rangle_E = \text{const} \sum_{x,y} e^{2\pi i \, n_{int} x/L_s} \langle L(0,0)L^*(x,y) \rangle. \quad (5.3)$$

Taking into account Eq. (4.1) for the point-point Polyakov loop correlator and summing over all momenta p_i in this equation we get[2]

$$\langle |L|^2 \rangle_E = \sum_{m \geqslant 0} \frac{C_m}{\cos(2\pi n_{int}/L_s) - \cosh(\sigma_m L_t)}. \quad (5.4)$$

Here the expansion over the excited mass states σ_m is written explicitly and the lowest state corresponding to the string

tension is $\sigma_0 = \sigma$. From Fig. 4 it follows that $\chi_L \ll \langle |L| \rangle^2$ for all β and n_E values. Thus the square root of Eq. (5.4) can serve as a good estimator for the Polyakov loop quantum average $\langle |L| \rangle$.

We use only the first two terms of the expansion (5.4) to fit the behavior of the *measured* Polyakov loop vs the external electric flux number. The corresponding fits for the confinement and deconfinement phases are shown in Figs. 5(a) and 5(b), respectively. The best fits for the string tension in the confinement phase (at $\beta = 1.6$) give $\sigma_0 = 0.167(13)$ and $\sigma_1 = 0.85(6)$. The value of σ_0 can be compared with the string tension without external field, $\sigma = 0.170(4)$. These values agree with each other within statistical errors. In the deconfinement phase ($\beta = 2.5$) the same picture is found: $\sigma_0 = 0.0096(5)$ and $\sigma_1 = 0.18(1)$, while the independent measurements at zero field lead to $\sigma = 0.0101(1)$. Therefore, the behavior of the Polyakov loop approximated via Eq. (5.4) in the external electric field is consistent with the string tension measurements at zero field.

So, in the case of nonvanishing external electric field, the bulk Polyakov loop expectation value may vanish regardless of the value of the actual string tension. Indeed, even at $\sigma = 0$ (which is not accessible on the finite lattice due to finite volume effects) the squared Polyakov loop expectation value (5.4) is decreasing when turning on the external electric flux. As we have mentioned in Sec. IV the influence of the external field on the Polyakov loop correlations is absent provided
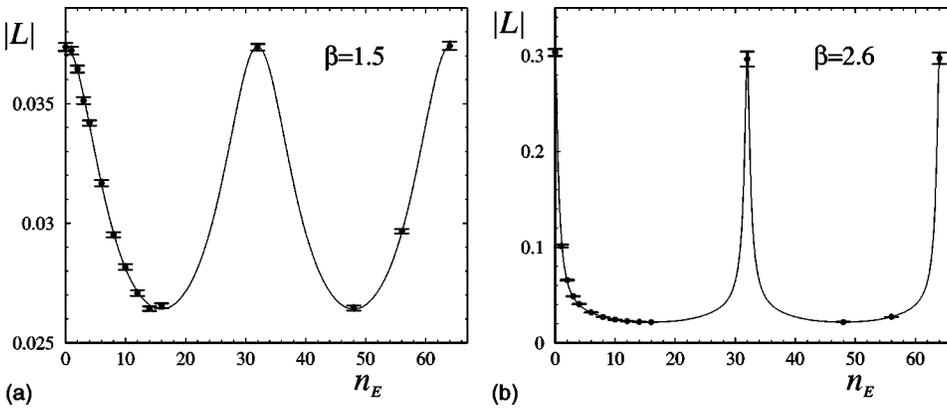

FIG. 5. The absolute value of the bulk Polyakov loop (5.1) vs the external electric flux n_E and its fit by formula (5.4) in (a) the confinement phase ($\beta = 1.6$) and (b) the deconfinement phase ($\beta = 2.5$).

---

[2]According to our considerations above, the dominating internal flux is equal to the external flux in the vicinity of the phase transition and thus we can safely put $n_{int} = n_E$.
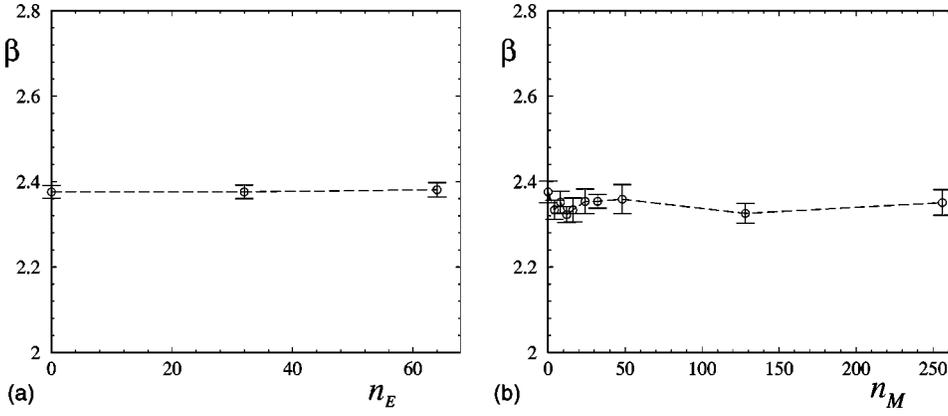
FIG. 6. Phase diagrams in the $n_{E/M}$-β plane derived from the module of the Polyakov loop for (a) electric and (b) magnetic fields, respectively.

the condition (4.9) for the internal flux n_{int} is fulfilled. Now, a similar effect is observed for the Polyakov loops themselves: the corresponding values for $n_E = n_{\text{int}} = 32, 64$ clearly coincide with $n_E = 0$ data. Thus we conclude that the observables based on the Polyakov loops may have a usual physical sense only in the cases of the quantized internal field (4.9).

Analogously, Figs. 4(a) and 4(b) show that the dependence of the Polyakov loop and its susceptibility on the coupling constant β are the same (within errors) for $n_E = 0, 32, 64$. The peaks in susceptibility may serve as good indicators of the (pseudo)critical coupling constant. At these distinguished values of the external electric field we have fitted the susceptibility near its maximum by the following function:

$$\chi_L^{\text{fit}}(\beta) = \frac{c_1^2}{c_2^2 + (\beta - \beta_c)^2}, \qquad (5.5)$$

where c_i and β_c are fitting parameters. The results are shown in Fig. 6(a) in the n_E-β plane. One can see that the influence of the external field on the critical temperature is negligible.

B. Magnetic field

The tree level contribution to the Polyakov loop observables is absent in the case of the external magnetic field. This is confirmed by Figs. 7(a) and 7(b) where the Polyakov loop and its susceptibility are shown as functions of β, respectively. The data points for all considered values of the external magnetic flux coincide with each other within errors. We

fit the Polyakov loop susceptibility by Eq. (5.5) to get the (pseudo)critical couplings. The corresponding phase diagram is shown in Fig. 6(b) in the n_M-β plane. One sees that the phase transition points are insensitive to the strength of the external magnetic field.

It is interesting to note that in non-Abelian gauge theories in $3+1$ dimensions the situation is quite different [13]. Here the position of the deconfining phase transition depends strongly on the strength of the applied magnetic field. The simplest, somewhat naive explanation of this fact could be as follows. In the non-Abelian gauge theory the coupling between gauge fields is stronger than in the Abelian theory. In particular, there is a correlation between spatial and temporal components of the fields which may imply that the external magnetic field (encoded in the spatial components) induces internal electric fluxes on the quantum level. As we have seen the electric fluxes strongly influence the Polyakov loop correlators generating the effective string tension (4.8). Contrary to the Abelian case this influence is not merely a classical (or, just inherent to the way of introducing the external field) but a real quantum effect.

In the next section we study the effects of the external fields on the agents of confinement, the Abelian monopoles, to explain the observed behavior of the system. A similar study for the non-Abelian gauge theory is underway [24].

VI. MONOPOLE PROPERTIES

The basic quantity to describe the behavior of the monopoles is the monopole density,
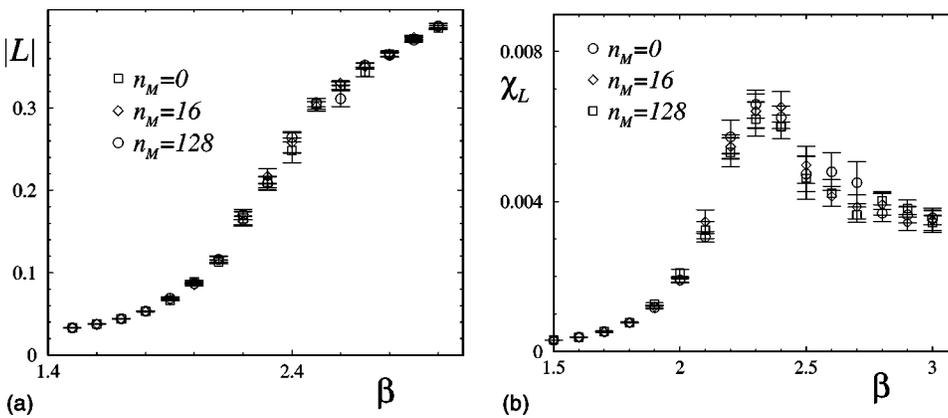

FIG. 7. (a) The Polyakov loop and (b) its susceptibility at various values of the external magnetic field n_M vs β.
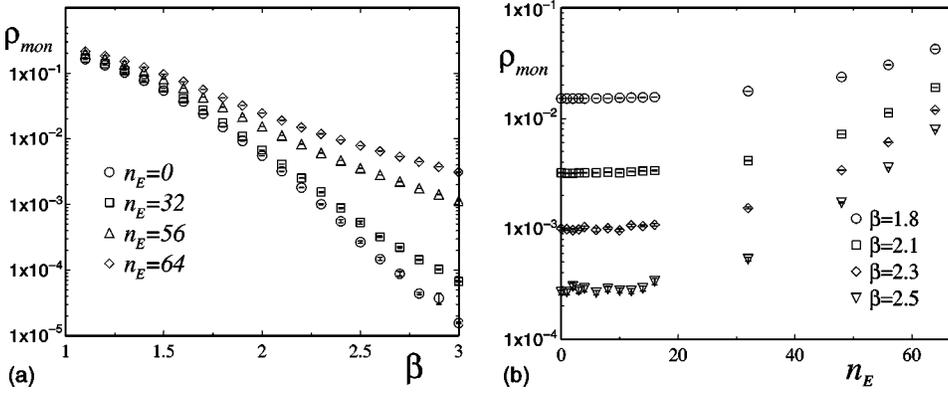
FIG. 8. Monopole density ρ_{mon} (a) vs β for various external electric fluxes, n_E, and (b) vs n_E for various β values.

$$\rho_{\text{mon}} = \sum_c |m_c|, \qquad (6.1)$$

where m_c is the integer valued monopole charge inside the cube c defined in the standard way [25]:

$$m_c = \frac{1}{2\pi} \sum_{P \in \partial c} (-1)^P [d\theta]_{\text{mod } 2\pi}. \qquad (6.2)$$

In our previous study [7] we have demonstrated that the monopoles are sensitive to the phase transition in the compact Abelian gauge model at finite temperature. Although in $(2+1)$D we have magnetic and electric fields among the three components of the field strength tensor, the sources of the respective fluxes will be simply called "monopoles" or "magnetic charges" in the following.

The mechanism which drives the finite temperature deconfinement phase transition is monopole binding. In the zero temperature case the plasma of monopoles and anti-monopoles can explain the permanent confinement of oppositely charged electric test charges [1] in bound states, kept together by a linear potential. Confinement appears due to the screening of the magnetic field induced by the electric current circulating along the Wilson loop. Monopoles and antimonopoles form a polarized sheet of finite thickness ("string") along the minimal surface $|A|$ spanned by the Wilson loop. The formation of the string leads, for nonvanishing electric current, to an excess of the free energy equal to $\sigma|A|$.

At finite temperature, dipoles are formed both in the confinement and deconfinement phases. In the deconfinement phase tightly bound dipoles dominate in the vacuum. The dipole plasma is inefficient to completely screen the field created by the electric currents running along the pair of Polyakov loops. This explains the absence of confinement in this phase.

Besides measuring the density of monopoles, we have studied the properties of the monopole ensembles by investigating the structure of monopole clusters. Clusters are connected groups of monopoles and antimonopoles, where each object is separated from at least one neighbor belonging to the same cluster by a distance less then or equal to R_{max}. In the following we use $R_{\text{max}} = \sqrt{3}\, a$ which means that neighboring monopole cubes should share at least one single

corner.[3] The increase of the coupling constant leads not only to an increase of the temperature, Eq. (2.3), but also to a decreasing lattice spacing a, Eq. (2.2). Thus at different β the same characteristic distance R_{max} corresponds to different physical scales. Therefore our results presented here are of a qualitative nature.

In our study without external field we have found that the dipoles are oriented dominantly in the temporal direction. At the confinement phase transition mostly clusters with two constituents or single monopoles and antimonopoles were observed. Decreasing further the temperature (or β), the monopoles become dense and start to form connected clusters (on a coarser and coarser lattice) containing various numbers of monopoles and antimonopoles. The largest clusters have been found to be more and more spherical. Finally we observed that only charged monopole clusters in the plasma (mainly individual monopoles) are needed to explain the measured string tension and, therefore, are responsible for confinement.

A. Electric field

To begin, we plot in Fig. 8(a) the total monopole density ρ as function of the coupling β for various values of the external electric flux n_E. The monopole density is a decreasing function of β at any value of the external field. However, ρ increases as the function of the strength of the applied external field, Fig. 8(b). The effect of the external field is very essential: the monopole density is increased up to almost two orders of magnitude (depending on the temperature) for the largest external flux values (compared to the system at zero external field).

However, an increased total monopole density does not mean in general that the confining properties of the system are enhanced. Only charged monopole clusters in the plasma state contribute to the string tension between electrically charged test particles. Tightly bound monopole pairs are not expected to contribute to the string tension. Therefore, we use our cluster labeling algorithm to look into the structure of the monopole ensemble. In Figs. 9(a) and 9(b) we show

---

[3]In Ref. [26] a similar definition has been used to investigate tightly packed clusters with $R_{max} = a$. In our case the condition for the cluster is more relaxed.
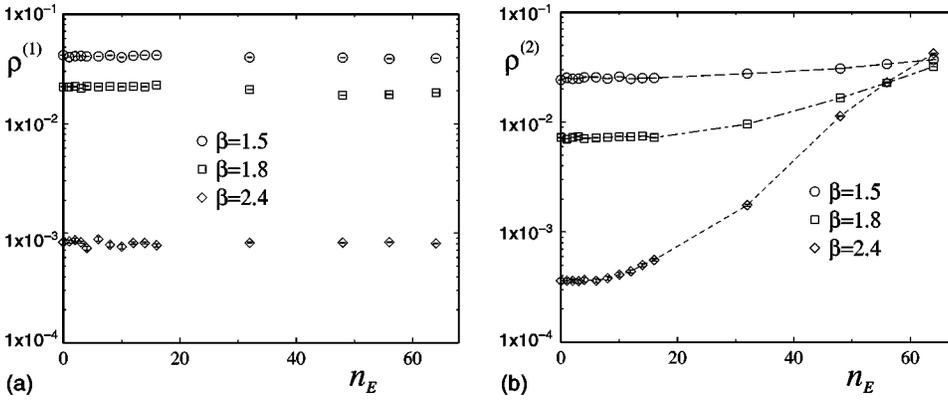
FIG. 9. The density of clusters of size (a) $N=1$ (single monopoles and antimonopoles) and (b) $N=2$ (dipoles) vs external electric flux n_E at various values of β.

how the densities of single monopoles [clusters made of just one (anti)monopole] and of dipoles (clusters made of two oppositely charged objects), respectively, depend on the strength of the external electric field.

One clearly sees that the plasma component of the single monopole ensemble does not feel the electric field at all. Thus the confining properties of the system should not depend on the external electric field in agreement with the conclusions made in the previous sections.

On the other hand, the dipole density changes drastically with increasing external field: the field creates the magnetic dipoles from the vacuum. Note that the larger the temperature (or, equivalently, β), the larger the increase of the dipole density. This fact is connected with the screening of the external fields inside the medium discussed in Sec. III. The larger the temperature, the larger the fields inside the medium. As a result, the effect of the external field becomes stronger with increasing temperature.

In a nonzero electric field the system is anisotropic in all directions. The electric field is directed along the y axis; the

"temperature" direction, z, is influenced by compactification. Therefore, we have to expect that the average sizes of the dipoles in different directions are not the same. At zero or small external field the dipoles are mainly directed along the temporal axis [7].

Increasing the external field, the dipoles are expected to become elongated along the direction of the applied field. Moreover, we have observed in Sec. III that the strength of the internal field inside the medium relative to the external field increases as a function of the coupling β. Thus the elongation of the dipoles in the field direction should increase with β.

All these effects are demonstrated in Fig. 10 using ellipsoids, the axes of which are equal to the average dipole sizes in the x,y, and z directions. In Fig. 10(a) we show how the mean dipole anisotropy changes with increasing external electric flux at fixed $\beta=1.8$ (in the confinement phase). Figure 10(b) demonstrates the dependence of the ellipsoids on β at fixed flux n_E. For convenience the projections of the ellipsoids onto the x-y and x-z planes are also shown.
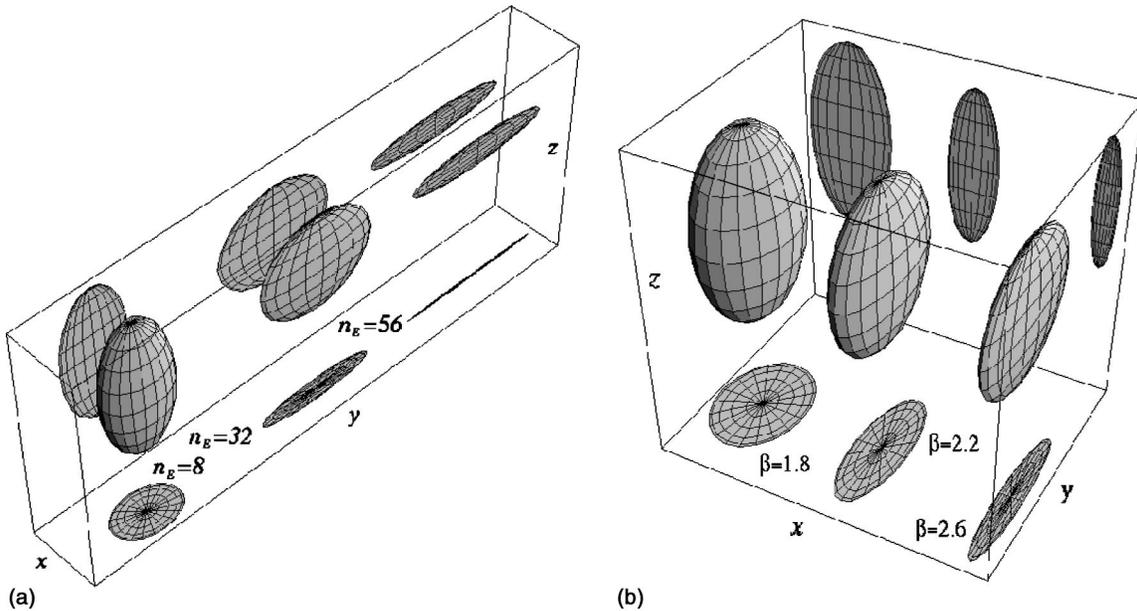

FIG. 10. The mean dipole anisotropy for increasing values of (a) the external electric flux n_E at fixed $\beta=1.8$, and (b) β at fixed n_E.
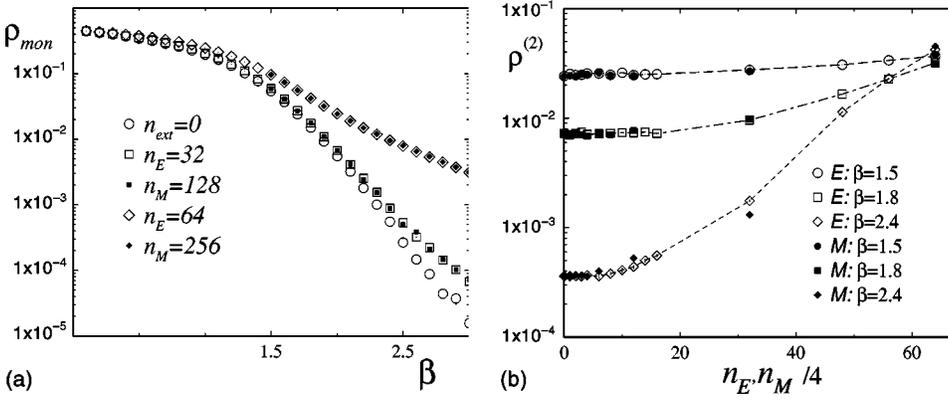
FIG. 11. (a) Total monopole density ρ_{mon} vs β for various external flux values n_{ext}. (b) Density of dipole clusters vs $n_{\mathrm{ext}} = n_E = n_M/4$ for some β values.

B. Magnetic field

The influence of the magnetic field on the monopole densities is very similar to that of the electric field. In Figs. 11(a) and 11(b) we present the measured total monopole density and the dipole density, as functions of β and the external fluxes, respectively. To compare the measurements for magnetic fluxes with those at nonzero external electric field, we note that for our lattice geometry the strengths of the magnetic and electric fields are equal to each other provided $n_M = 4n_E$. According to those figures both total monopole density and dipole density do not depend on the type of the external fields if the field strengths are the same. We have checked that the single monopole density coincides for magnetic and electric fields of the same strength as well. Thus the cluster structure does not depend on whether the external field is of electric or magnetic kind.

The mean dipole anisotropy depends on the *type* (direction) of the external field. We show the behavior of this quantity in Figs. 12(a) and 12(b) for increasing external magnetic field and β, respectively. In the external magnetic field the system is symmetric in the x and y directions. The dipoles become more elongated in the (temporal) z direction for stronger external magnetic fields. Increasing the coupling β leads to a larger anisotropy since the medium does not screen the external field in the deconfinement (large β).

The orientation properties of the dipoles influence the resulting electromagnetic fields in the medium, Fig. 1. According to Figs. 10(a) and 12(a) the stronger the external field, the larger the elongation of the dipoles in the direction of the field. In turn this increases the dipole momenta in the direction of the applied field and, as a result, leads to an enhanced screening of the external fields by the media. This effect is clearly observed in Fig. 1.

Another interesting effect due to the dipole orientation is the clear difference in screening for strong magnetic and electric fields of equal strength in the deconfinement phase, Fig. 1. According to Fig. 11(b), the dipole densities for both cases are the same. Since $L_t < L_s$, the dipole magnetic moment density projected to the magnetic field direction is larger than the corresponding quantity for the electric field direction. On the other hand, the larger the dipole moment density inside the medium, the stronger the field attenuation. Thus at strong external fields the screening must be more effective for magnetic fields compared to electric fields. This
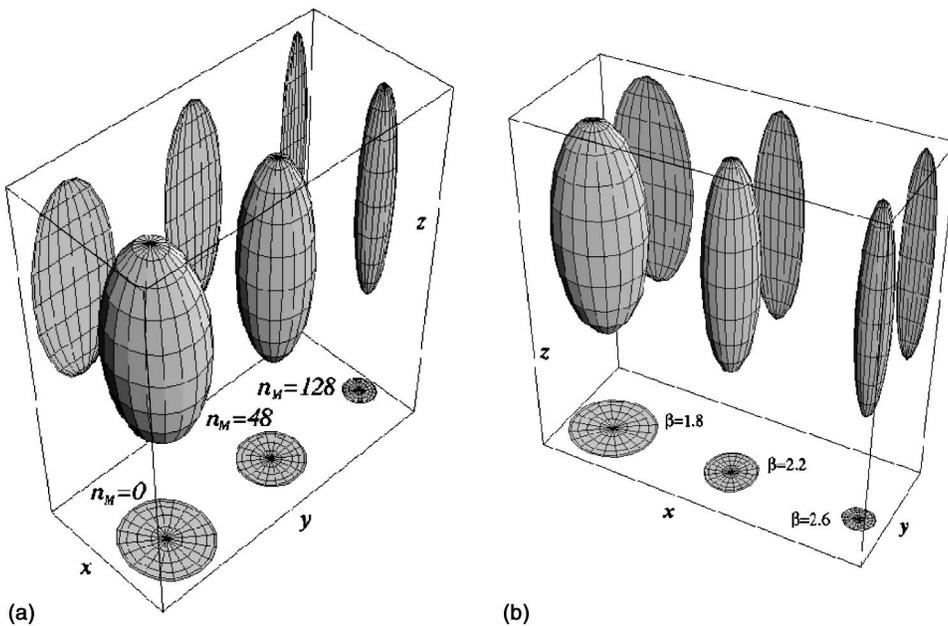

FIG. 12. The mean dipole anisotropy for increasing values of (a) the external magnetic flux n_M at fixed $\beta = 1.8$ and (b) β at fixed n_M.

mechanism works at high temperatures (large β) where the dipole fraction is dominant [cf. Figs. 9(a) and 9(b)].

VII. CONCLUSIONS

We have investigated the properties of the 3D compact electrodynamics at finite temperature in external constant electric and magnetic fields. The main result is that the deconfinement temperature is insensitive to both electric and magnetic external fields. We have found the reason for this behavior in terms of the monopole degrees of freedom: the external fields create tightly bound magnetic dipoles (monopole-antimonopole bound states) from the vacuum while the density of unpaired monopoles (which are responsible for the confinement of electric charges) stays unchanged. This result is not obvious from the beginning since another option is possible: the external fields could destroy the monopole bound states enforcing confining properties of the medium. This is not the case.

At zero external fields the magnetic dipole states are more elongated in the temperature direction. The external magnetic field which is parallel to the temperature direction makes this elongation stronger. However, an external electric field turns the dipoles to the corresponding spatial direction. The effects of the external field on the medium are stronger in the deconfinement phase in which both electric and magnetic external fields are not screened.

We have also shown that the external electric field influences the Polyakov loop classically (or, in other words, on tree level). This leads to a vanishing Polyakov loop and, in certain cases, to a nonvanishing "effective string tension" (4.8) depending on the external field (being in deconfinement at zero field). However, this behavior of the Polyakov loop does not indicate a restoration of confinement for certain external field fluxes. At special flux values [for which the internal electric field is quantized according to Eq. (4.9)] both the Polyakov loop expectation value and σ_{eff} coincide with the values at zero external field.

The string tension (correctly defined from the correlation function of Polyakov plane-plane correlators parallel to the external electric field in the spatial direction) is not influenced by the external electric field and coincides with the zero-field value. The tree level effects on Polyakov loops and Polyakov loop correlation functions are absent for external magnetic fields pointing in the timelike direction.

The dynamics of the Abelian system is different from the behavior of the $(3+1)$D non-Abelian gauge theory. The authors of Ref. [13] have found that the external magnetic field increases the deconfinement temperature contrary to our results in $(2+1)$D compact Abelian gauge theory. The reason for this difference may lie in the different behavior of the monopoles in the Abelian and non-Abelian gauge theories. The investigation of the monopole properties in the non-Abelian gauge theory is underway [24].

ACKNOWLEDGMENTS

[1] A.M. Polyakov, Nucl. Phys. **B120**, 429 (1977).

[2] M. Göpfert and G. Mack, Commun. Math. Phys. **82**, 545 (1981).

[3] B. Svetitsky, Phys. Rep. **132**, 1 (1986).

[4] P.D. Coddington *et al.*, Phys. Lett. B **175**, 64 (1986).

[5] N. Parga, Phys. Lett. **107B**, 442 (1981).

[6] J.M. Kosterlitz and D.J. Thouless, J. Phys. C **6**, 1181 (1973).

[7] M.N. Chernodub, E.-M. Ilgenfritz, and A. Schiller, Phys. Rev. D **64**, 054507 (2001).

[8] M.N. Chernodub, Phys. Rev. D **63**, 025003 (2001); Phys. Lett. B **515**, 400 (2001); B.L. Bakker, M.N. Chernodub, and A.I. Veselov, *ibid.* **502**, 338 (2001); I.I. Kogan, A. Kovner, and B. Tekin, J. High Energy Phys. **03**, 021 (2001).

[9] N.O. Agasian and K. Zarembo, Phys. Rev. D **57**, 2475 (1998).

[10] G. Dunne, I.I. Kogan, A. Kovner, and B. Tekin, J. High Energy Phys. **01**, 032 (2001).

[11] T. Schäfer, E.V. Shuryak, and J.J.M. Verbaarschot, Phys. Rev. D **51**, 1267 (1995); R. Rapp, T. Schäfer, E.V. Shuryak, and M. Velkovsky, Ann. Phys. (N.Y.) **280**, 35 (2000); E.-M. Ilgenfritz and E.V. Shuryak, Phys. Lett. B **325**, 263 (1994).

[12] N.O. Agasian, Phys. Lett. B **488**, 39 (2000); I.A. Shushpanov and A.V. Smilga, *ibid.* **402**, 351 (1997); A.I. Vainshtein *et al.*, Sov. J. Nucl. Phys. **39**, 77 (1984); R. Brower, P. Rossi, and C. Tan, Nucl. Phys. **B190**, 699 (1981).

[13] P. Cea and L. Cosmai, Phys. Rev. D **48**, 3364 (1993); hep-lat/0101017.

[14] M.N. Chernodub, F.V. Gubarev, and E.-M. Ilgenfritz, Phys. Lett. B **424**, 106 (1998); M.N. Chernodub, F.V. Gubarev, E.-M. Ilgenfritz, and A. Schiller, *ibid.* **443**, 244 (1998); **434**, 83 (1998).

[15] K. Kajantie *et al.*, Nucl. Phys. **B544**, 357 (1999); D. Comelli, D. Grasso, M. Pietroni, and A. Riotto, Phys. Lett. B **458**, 304 (1999); V. Skalozub and M. Bordag, Int. J. Mod. Phys. A **15**, 249 (2000).

[16] P. Cea and L. Cosmai, Phys. Rev. D **48**, 3364 (1993).

[17] P. Dimopoulos, K. Farakos, and G. Koutsoumbas, Phys. Rev. D **63**, 054507 (2001).

[18] J. Alexandre *et al.*, Phys. Rev. D **64**, 034502 (2001); K. Farakos *et al.*, *ibid.* **61**, 045005 (2000); V.P. Gusynin, V.A. Miransky, and I.A. Shovkovy, *ibid.* **52**, 4747 (1995); Phys. Rev. Lett. **73**, 3499 (1994); **76**, 1005(E) (1996).

[19] P.H. Damgaard and U.M. Heller, Nucl. Phys. **B309**, 625 (1988).

[20] P. Cea and L. Cosmai, Phys. Rev. D **60**, 094506 (1999).

[21] P. Cea and L. Cosmai, Phys. Rev. D **43**, 620 (1991).

[22] J. Glimm and A. Jaffe, Commun. Math. Phys. **56**, 195 (1977).

[23] J. Engels, V.K. Mitrjushkin, and T. Neuhaus, Nucl. Phys. **B440**, 555 (1995).

[24] M. N. Chernodub, E.-M. Ilgenfritz, and A. Schiller (in preparation).

[25] T.A. DeGrand and D. Toussaint, Phys. Rev. D **22**, 2478 (1980).

[26] Z. Schram and M. Teper, Phys. Rev. D **48**, 2881 (1993).